DOI: 10.31534/engmod.2024.2.ri.04f
Original scientific paper
Received: 19.03.2024.

Multi-Objective Optimisation-Oriented Model of an Air-Conditioned Environment

Oscar Daniel Chuk[1], **Gustavo Rodriguez Medina**[1], **Bruno Damián Arballo**[2], **Ernesto Kuchen**[2]

[1] *Facultad de Ingeniería, Universidad Nacional de San Juan, ARGENTINA*
e-mails: dchuk@unsj.edu.ar; grodriguez@unsj.edu.ar

[2] *CONICET and Facultad de Arquitectura, Urbanismo y Diseño, Universidad Nacional de San Juan, ARGENTINA*
e-mails: arballobruno@gmail.com; ernestokuchen@gmail.com

SUMMARY

A dynamic modelling of a workplace in an area with high temperature and low humidity in the summer is described. The aim is to subsequently use the model to apply multi-objective predictive supervision of the environment climate. Two main variables are modelled: thermal comfort and energy consumption. First, a model of the different temperatures, humidity levels and the behaviour of the air-conditioning system is created. These variables respond to two control actions: the setpoint of the air-conditioning system and the speed of an airflow that may come from outside, and to a disturbance, the external temperature. The overall model is disintegrated into sub-models that precisely describe the internal influences between the variables.

This model provides new insights on the subject in that it correctly describes the dynamic behaviour of the system by using simple Linear Parameter Varying descriptions to model the non-linear relationships, incorporates humidity into the thermal comfort model, includes forced ventilation of outside air as a strategy to reduce electricity consumption, defines a relative power unit that simplifies the measurement of electrical consumption, and its methodology is easy to apply to other environments. Different experiments demonstrate that the model obtained accurately depicts the actual variables.

KEY WORDS: *Dynamic model; air-conditioning; thermal comfort; energy consumption; multi-objective predictive supervision.*

1. INTRODUCTION

The total energy consumed in heating, ventilation and air-conditioning (HVAC) systems in commercial and residential buildings nowadays accounts for 40% of global energy consumption (37% in Argentina) and causes more than 36% of CO2 eq. emissions [1]. Optimizing energy consumption while maintaining thermal comfort conditions for users has then become a priority. This paper deals with the development of a dynamic model that describes the variations

in thermal and humidity factors within a workspace located in the Faculty of Engineering at the National University of San Juan (UNSJ), an arid zone of Argentina, during the summer season. The climate in this city is continental, with high temperatures and low humidity in summer, as described in the national standard IRAM 11603 [2]. The main variables to be modelled are the user´s thermal comfort and the energy consumption of the HVAC system.

The final goal is to implement a Multi-objective Predictive Optimizing Control of the air conditioning system [3]. This type of supervisory control performs multi-objective optimisation [4] since it considers factors that normally compete with each other, such as user comfort and energy consumption. It performs this optimization with a Model Predictive Control (MPC) strategy [5], that is, running the model forward in time in order to calculate the optimal control actions. A well-suited model is the main challenge when implementing predictive control, especially when applying it to comfort and energy efficiency [6].

Different models describing how buildings react to external variables and climate control are discussed in reviews such as those by Afram and Janabi-Sharifi [7] and Homod [8].

The models are frequently classified as white, grey, and black box models based on their level of transparency. Arendt et al. [9] have carried out an appropriate comparative analysis of these modelling criteria for the simulation of the thermal behaviour of educational buildings. Similar classifications using different terminology have also been established. Hensen [10], for example, defines four levels of models, from a Conceptual one, in which an ideal plant is considered, to an Explicit one, which has precise knowledge of the different subcomponents of the system in terms of energy balance. The traditional black and white box models can be identified with these extremes.

In a white box model, the internal details and underlying mechanisms of the system being modelled are known and taken into account. It requires a comprehensive knowledge of the physics involved, the components used and the boundary conditions of the modelled object. Normally, the changes over time are determined by solving the differential equations that explain the process using numerical methods.

White box models have been widely used in environment modelling. For example, Muñoz et al. [11] used the admittance method to thermally characterize multilayer wall materials. Tashtoush et al. [12] present a dynamic model of an air-conditioned space that includes the physical details of the space, heating, cooling and dehumidifying coils, humidifier, ductwork, fan and mixing box. Commercial software packages like ESP-r and TRNSYS [13] are commonly used to predict the thermal performance of buildings. These programs have been developed with a deep understanding of the physics and materials used. Assessing alternatives for retrofitting environments and HVAC systems is another valuable application for these programs [14]. On the other hand, white box models have the disadvantage that they require a precise knowledge of the physical parameters of the different elements involved. The incorrect parameters can lead to significant differences between the actual behaviour of the system and the behaviour described by the model. This has been emphasized by authors like Akkurt et al [15]. Some researchers also argue that the calibration of these models in the case of complex buildings is cumbersome so the application of predictive control is only possible for simple environments [16]. For these reasons, some authors such as Trcka and Hendsen [17] place this type of model in the category of models used for Building Energy Performance Simulation (BEPS), rather than in the category of models used for control and optimization.

At the other end of the spectrum, there is the black box model, which is named for its complete opacity. It is assumed that there is no knowledge of its internal structure, but it is based solely

on observations of input and output data (data-driven). The techniques used to construct these models usually stem from the field of artificial intelligence and are often based on genetic algorithms [18] and, in particular, neural networks [19].

One of the main advantages of black box models is that they do not require detailed knowledge of the system. These tools are also useful when dealing with variables that have complex interconnections. However, its drawbacks arise from a high dependence on the quality of the input data. When the data used to calibrate the model are not reliable or do not cover all possible situations, the results obtained may deviate significantly from reality. For the same reason, they are difficult to correct or modify.

Grey box models lie between the two types of models mentioned above. Some structural features of the model are assumed, such as the orders of the transfer functions and the internal influences between the different variables involved, and the parameters of these models are determined by analysing the input and output data.

The approach to a grey box model can follow two basic ideas:

1. Models can be based on physics equations, but instead of deriving their parameters from knowledge of the individual components, they are calibrated on the basis of recorded measurements.
2. Generic models with a certain structure, e.g., in state space or using linear or non-linear input/output transfer functions, can be adopted, and records of measurements over time can also be used to estimate model parameters.

In the latter alternative, different approaches can be considered. Among the most common are:

1. Linear state space models. These models are useful when the environment is modelled under relatively limited variations in the variables affecting the system (e.g., outdoor temperature), which allows the assumption of a linear relationship between inputs and outputs. State models represent the system intuitively when each state variable is identified with some determinant value of the system's behaviour. With this idea, Drgona [20] uses a fourth-order state model, where the state variables are the external facade temperature, the internal facade temperature, the floor temperature and the internal room temperature.
2. Fuzzy logic. Prior knowledge about the system is expressed in terms of labels and linguistic rules and the parameters of these rules are then identified [21].
3. Linear transfer functions, either in the continuous or discrete domain.
4. Non-linear descriptions. When the behaviour of variables is complex and cannot be properly described by linear models, it can be verified that non-linear relationships exist between them. A non-linear description can also take different forms, such as states or non-linear differential equations. In this work, a Linear Parameter Varying description (LPV) is used [22] because it is very effective and easy to understand for those who know the behaviour of the system, which facilitates the identification of the parameters.

Once the model structure is defined, the usual techniques for determining the model parameters include, among others, the frequency domain method, the maximum likelihood method, and, above all, the Prediction Errors Minimisation PEM method, which is performed using least squares. This criterion must be supplemented by other model quality metrics in non-linear cases. This applies to certain sub-models described under the LPV criterion, which are discussed in more detail below.

Grey box models tend to have slightly larger prediction errors than black and white box models. However, they are very suitable for implementing an MPC because at each sampling interval, the controlled variable is measured again and the model is re-run from that point, so it is not the exact value of the prediction that is important but its trend.

It is generally agreed that a simple grey box model is sufficient for implementing an MPC [6]. They are also more robust (less sensitive to parameter errors) and perform better when the operating conditions differ from those under which the parameters were calibrated.

Given these considerations, the following model was chosen for this work:

- Grey box dynamics.
- Of an ambient and its HVAC system in the post-occupancy phase.
- Aimed at multi-objective optimisation of user´s comfort and energy efficiency, in summer.
- Characterized by low-order transfer functions, albeit with significant pure delays.
- Most transfer functions are linear and, in some cases, LPV descriptions are used.

2. THE ENVIRONMENT, ITS HVAC AND RELATED VARIABLES

The set under investigation is shown schematically in Figure 1. The dimensions of the workspace are 7.2m long, 4.9m wide and 3.25m high and it is used for research and development tasks. The average occupancy rate is between 2 and 3 people for 6 hours on working days. As a boundary condition, it has a single wall -1- that is in contact with the outside world and lets in air and natural light through a window. As it faces south, it never receives direct sunlight. The other walls are connected to other workspaces and an indoor corridor, the ceiling to a room upstairs and the floor to the natural ground. All these conditions explain the good insulation and consequently the high time constants, in the order of hours, for the influence of the outside temperature on the internal variables. While the characteristics of the space primarily favour thermal comfort, the harsh summer conditions in this area require air conditioning, which consumes significant amounts of energy. It should also be noted that the system presents a challenge for automatic control as it has high pure delays with respect to the time constants involved.

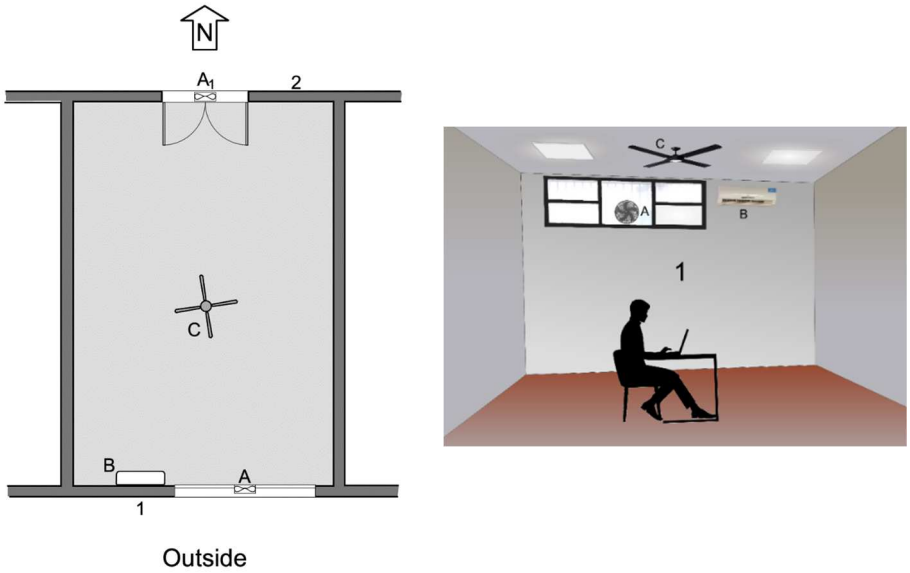

Fig. 1 *Ground plan and view to the south of the room under study and its air-conditioning devices*

The entrance to the workspace is located on Wall 2, opposite to Wall 1. A blower 'Fan A' located in the window on Wall 1, in conjunction with an exhaust fan over the entrance door on Wall 2, 'Fan A_1', forms a variable-speed forced ventilation system (with speed denoted as v_a), which draws in outside air and circulates it through the room along its longest axis. If outside air is not supplied, an additional ceiling fan, 'Fan C', also operating at variable speed v_a, can generate an indoor airflow. This ventilation system serves a dual purpose: it equalizes the temperatures in the room and improves the occupants' sense of comfort by promoting convective heat transfer from the body to the surrounding environment.

The HVAC unit B operates at 220V, 50Hz and has a split configuration and ON/OFF operation, like most HVACs in Argentina. It blows the air at 1000 m^3/h. The cooling power consumption is 1915W and has a cooling capacity of 6150W [23]; with these data, the Seasonal Energy Efficiency Ratio SEER [24,25] is 6150W / 1915W = 3.2, indicating that it is a mid-efficiency device. This underlines the idea of the need for optimisation, the ultimate goal of the project in which this study is embedded.

Three temperatures, the ambient humidity and the power consumption of the HVAC systems are measured and then modelled. The measured temperatures are the outdoor temperature T_e [°C], using a sensor located outside the Wall 1, the ambient temperature T_a [°C], measured at 1.1m above the floor [26] in the middle of the room (under the 'Fan C'), the mean radiant temperature T_{rm} [°C] [27], measured at the same location with a balloon temperature sensor, and the temperature associated with the HVAC unit T_{aa} [°C], measured with a sensor at the top air inlet of the HVAC unit, also near Wall 1, see Figure 2. The linear distance between the measurement points of T_{aa} and T_a is approximately 4m.

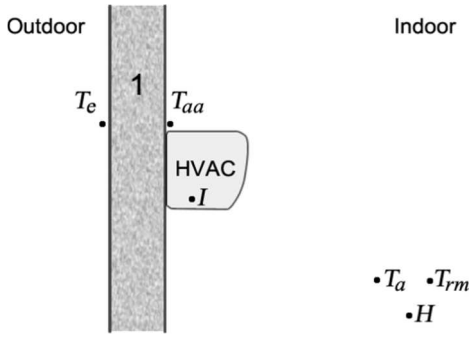

Fig. 2 *Relative position of the measurement points, not to scale*

The T_{aa} temperature measurement has a dual purpose: On the one hand, when the HVAC is in operation mode, it is equivalent to the temperature measured by the HVAC's inside sensor and is then used to predict when the compressor unit device will be in the ON or OFF state. On the other hand, this point indicates the internal temperature of Wall A when the HVAC is not operating. Other sensors could have been placed on each of the other walls, but as they behave adiabatically, this was sufficient to get a proper model.

Humidity H [%] is measured relatively, as the amount of water vapour in the air, expressed as a percentage of the maximum amount the air can hold. It is measured at the same point as T_{aa} and T_{rm}. The measurement of the current consumed I [A] by the HVAC is used for energy calculations.

3. MODEL DEVELOPMENT

The inputs of the entire model are the reference temperature (or setpoint) SP [°C] at which the HVAC operates, the air speed v_a [m/s] and the outdoor temperature T_e [°C] as a perturbation. See Figure 3.

The primary variables to be modelled, mentioned above in Section 2, allow the calculation of the variables relevant for the optimisation: the thermal comfort, expressed as the percentage of dissatisfied users *Disc*, and the energy consumption, expressed as a relative power P_r. Both will be formally defined later.

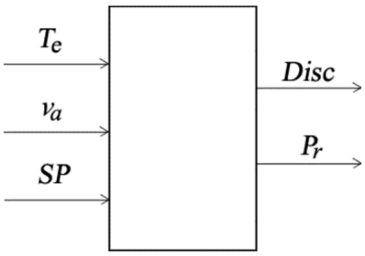

Fig. 3 *Block diagram of the whole room-HVAC system*

To obtain the sub-models presented below, various datasets obtained from different experiences of measuring signals over time were used. These covered the typical outdoor temperature ranges of the city in the summer season, between 15°C and 45°C, and different time evolutions of the outdoor temperature T_e, with increasing and decreasing daily averages. As is usual for dynamic models, identification was made with the dataset of one experience, using the data of another experience to validate the obtained model. The final model, achieved by iteration of this methodology, properly reproduces the behaviour of the variables for all the experiences included in the identification.

3.1 INFLUENCE OF THE OUTSIDE TEMPERATURE THROUGH THE ENVELOPE

The energy transfer through the envelope, without the operation of the HVAC, primarily affects the temperature associated with the inside of the wall T_{aa} and, thus, the other variables. The more detailed version of the block diagram of the model is outlined in Figure 4.

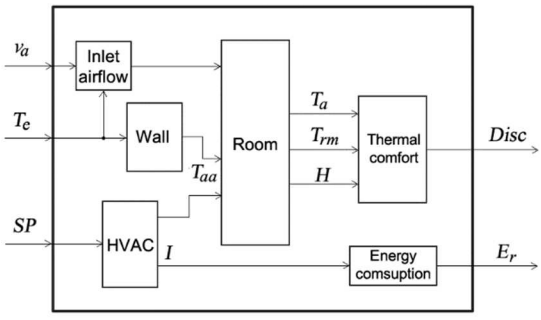

Fig. 4 *Block diagram with internal influences*

The change in wall temperature due to outside temperature, denoted as T_{aae}, was adequately described by a linear transfer function in the discrete domain with parameters obtained by PEM. With a sampling interval of 0.0667 min, it has the following form:

$$G_{aae} = \frac{T'_{aae}}{T'_e} = \frac{0.0000272\, z^{-150}}{1 - 0.7991\, z^{-1} - 0.2008\, z^{-2}} \quad (1)$$

In the identification process, an attempt was made to choose the lowest order of the model that maintains a bounded error, as in the following cases. Figure 5 shows the comparison between the measured variable and its model in an experiment of just over 3 days with typical variations in total outdoor temperature T_e between 10°C and 25°C.

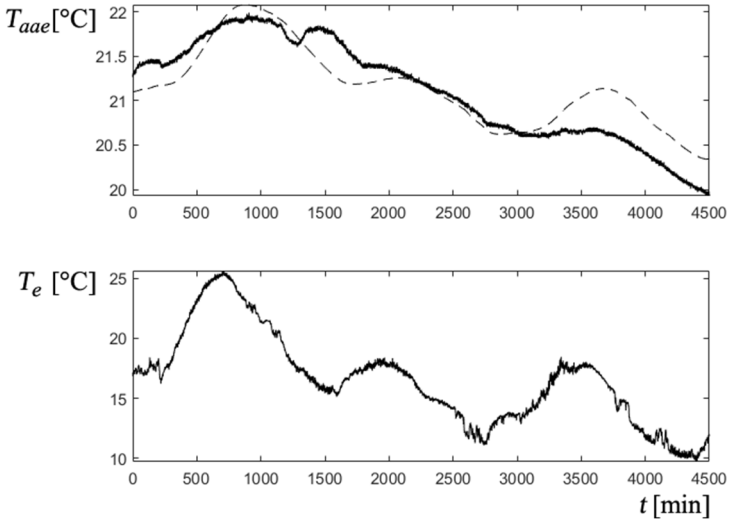

Fig. 5 *Influence of the outside temperature on the wall temperature; The filled line is the actual output and the dashed line is the model output*

The discrete transfer function G_{aae} acts on the differences between the two values T_{aa} and T_e with their mean values, denoted as T'_{aae} and T'_e. The average value of T_e is extracted using a high pass filter HPF, see Figure 6. To obtain the absolute value of the output, a constant value $\overline{T_{aa}}$ must then be added.

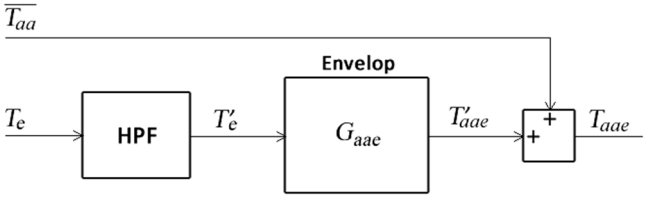

Fig. 6 *Block diagram of the model of the dependence of wall temperature on outdoor temperature through the envelope*

The combined effect of the pure delay and the time constants involved results in a total delay between input and output temperature peaks of about 4.5 hours for a daily sinusoidal input. See Figure 7.

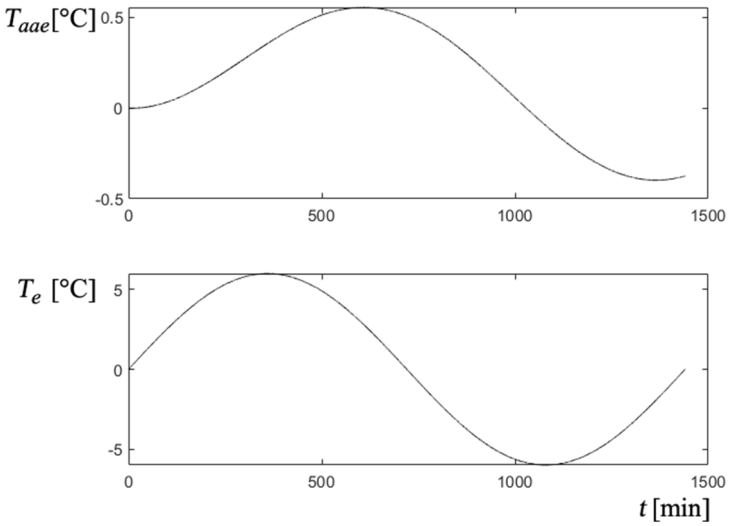

Fig. 7 *Response of the wall temperature model T_{aae} to a daily sine wave variation in T_e*

Similarly, the influence of the outside temperature on the ambient relative humidity H_e can also be determined.

$$G_{he} = \frac{H_e'}{T_e'} = \frac{0.000035\, z^{-150}}{1 - 1.338\, z^{-1} + 0.1624\, z^{-2} + 0.1759 z^{-3}} \quad \textbf{(2)}$$

The block diagram has the same structure as the temperature diagram in Figure 6. The comparison between the actual output and the model is depicted in Figure 8.

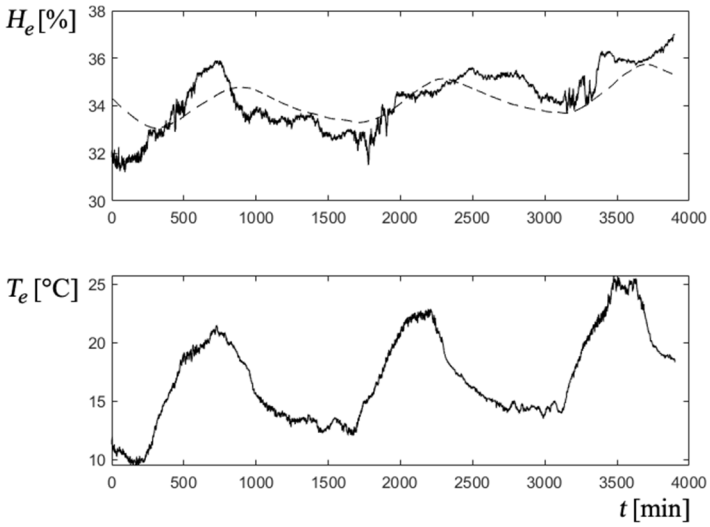

Fig. 8 *Response of the Humidity model (dashed line) in relation to the outdoor temperature*

3.2 INFLUENCE OF OUTSIDE TEMPERATURE THROUGH FORCED CROSS VENTILATION

This ventilation occurs when the outside air enters through Fan A in Figure 1 and exits through its counterpart exhaust fan located on the opposite wall. Modelling this influence is important because as long as the outdoor temperature is lower than the indoor temperature (mainly at night), significant temperature reductions can be achieved to reduce energy consumption during the day.

The following identifications of the influence of the outside air flow on temperatures and humidity are presented in the same experience, in order to be able to make an appropriate comparison.

3.2.1 INFLUENCE ON WALL TEMPERATURE T_{aa}

The following observations can be made when testing with different air velocities (Figure 9).

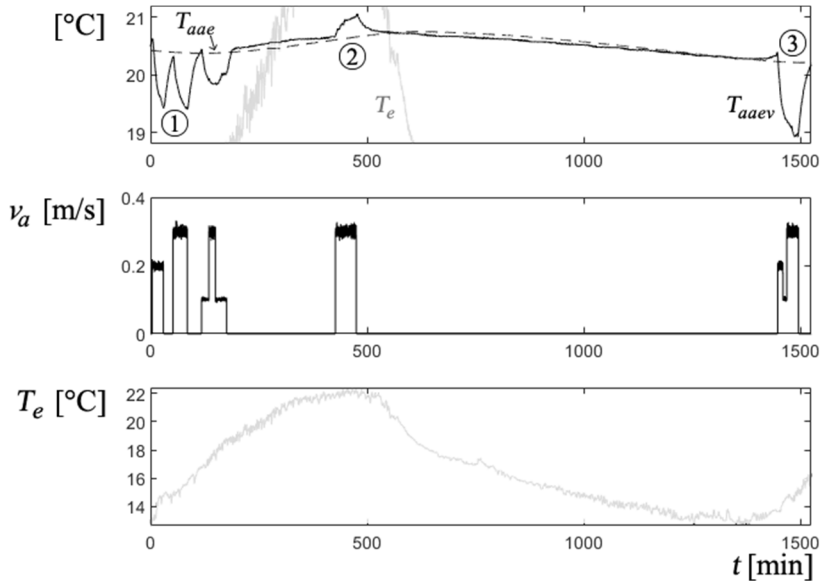

Fig. 9 *Influence of the outside temperature (grey line) on the wall temperature due to forced ventilation*

1. Looking at the behaviour of the wall temperature due to the combination of the external temperature and the air velocity T_{aaev}, compared to that which depends only on the external temperature T_{aae} through the envelope (identified in the previous point and plotted here in dashed line), it follows that it increases when $T_e > T_{aae}$ (state 2 in the graph) and decreases the other way round (states 1 and 3). This makes sense. When warmer outside air is brought into the room through the ventilation, the internal temperature tends to rise, and vice versa. This suggests that the influence of the outside temperature by the air supplied from outside G_{aaev} should be modelled as a function of the $T'\Delta_{eaa}$ difference between T_e and T_{aae} and then added to the latter. See Figure 10. This considers the effect of external ventilation.

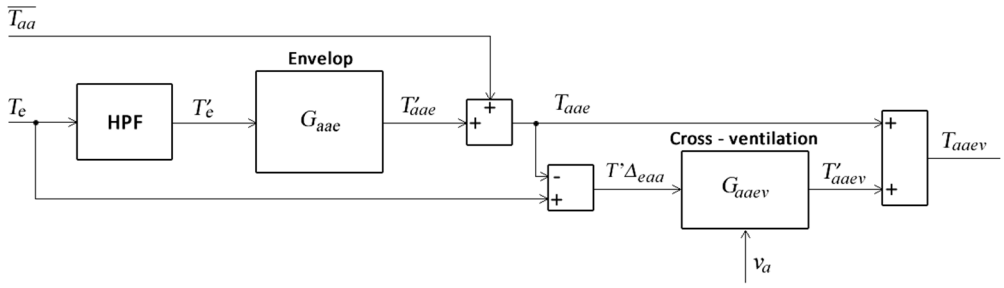

Fig. 10 *Block diagram showing the influence of the outside temperature on the wall temperature, both through the envelope and the forced cross-ventilation*

2. The experiment in Figure 9 also shows a predictable effect of air speed v_a in which the outside temperature affects the other variables. Not only does the effect of T_e on T_{aa} increase with air speed, suggesting a dependence of the static G_{aaev} gain on this variable. In addition, the time constants involved also vary with different v_a rates. Taking this into account, G_{aaev} was modelled as a first-order system with pure linear delay with linear variant parameters LPV, where the three parameters of the model, K_{av}, tg_{av} and tu_{av}, are dependent on v_a.

$$G_{aaev}(s) = \frac{T'_{aaev}(s)}{T\Delta'_{eaa}(s)} = \frac{K_{av}(v_a)\ \mathrm{e}^{-tu_{av}(v_a)\,s}}{1+\ tg_{av}(v_a)\,s} \tag{3}$$

   In this case, the model is expressed in continuous time. This makes it easier to determine the parameters as a function of v_a.

Among all possible representations of the model parameters (3) as a function of the scheduling variable v_a (fuzzy, point interpolation, neural networks, etc.), a second-order polynomial form was chosen due to its simplicity.

Since this is a non-linear system, the PEM error minimisation criterion [28] must be supplemented by tests of independence and whiteness validity and other indicators of model quality to identify the parameters of these parabolas [29,30]. These are combined using a multi-objective strategy [31,32]. Using this technique, the variation of the first-order model parameters with v_a was determined as shown in Figure 11.

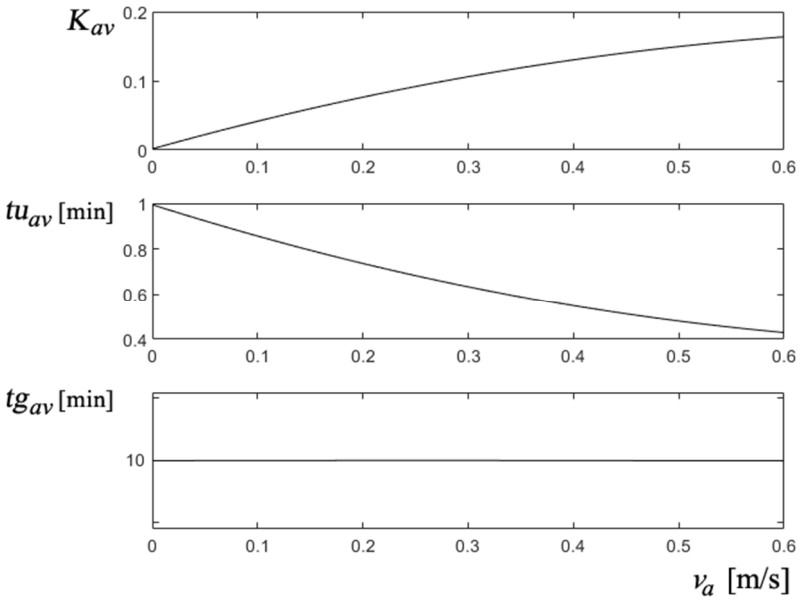

Fig. 11 *First-order LPV parameters of the outdoor temperature under the influence of forced cross-ventilation*

It can be observed that, as expected, there is no external thermal contribution at null air speed v_a, and the pure delay in sensing a change also decreases with speed. The fact that the time constant of the system is almost invariant is not so easy to predict. With these parameters, the model shown in Figure 10 behaves as shown in Figure 12.

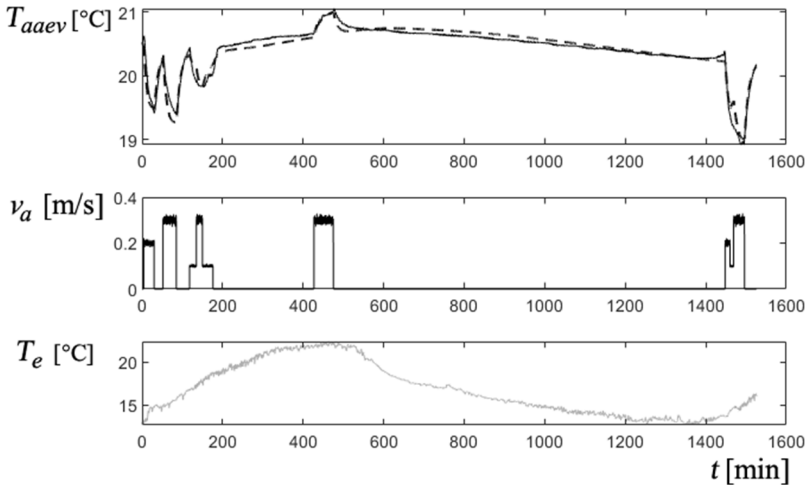

Fig. 12 *Model behaviour of the outdoor temperature under the influence of cross ventilation (dashed line)*

The influence of the outside temperature through cross-ventilation v_a on the ambient temperature T_a and the mean radiant temperature T_{rm} is obtained similarly.

3.2.2 INFLUENCE ON THE AMBIENT RELATIVE HUMIDITY *H*

When analysing the behaviour of the humidity with the external airflow, it can be seen that it also depends on the difference $T'\Delta_{eaa}$ between T_e and T_{aae}, but in the opposite direction: if this signal is positive, the humidity level will decrease and vice versa. This leads to the conclusion that it can also be described by a first-order LPV system G_{hev} similar to the one previously described, having a transfer function with the same structure as (2). The corresponding block diagram is drawn in Figure 13, and the temporal behaviour of the model in Figure 14. The evolution of the G_{hev} parameters with air velocity exhibits similar parabolas to those of the temperature shown previously in Figure 11 but with negative gains.

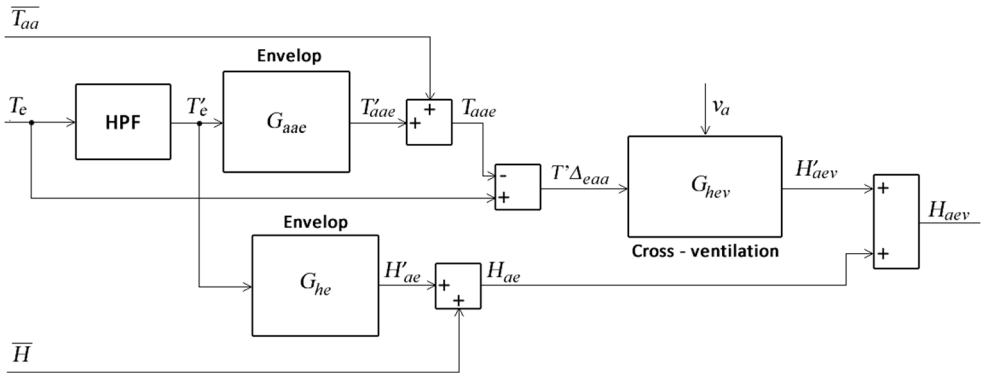

Fig. 13 *Block diagram illustrating the influence of the outdoor temperature on humidity, both through the envelope and through forced cross-ventilation*

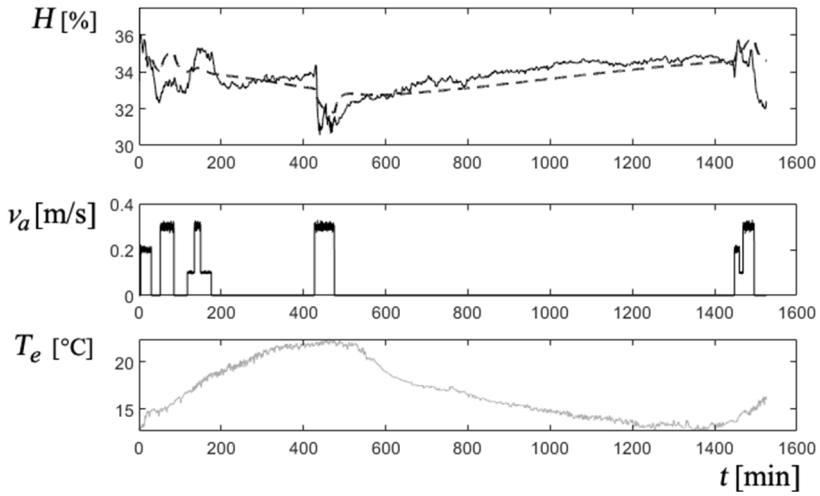

Fig. 14 *Behaviour of the humidity model (dashed line) with the outdoor temperature, through forced cross-ventilation*

3.3 OPERATION OF THE AIR-CONDITIONING SYSTEM

Looking at a typical test of the variables against reference changes in the HVAC, as shown in Figure 15, the following observations can be made.

1. The speeds at which the different variables move seem to depend on the operating range defined by the reference or setpoint *SP* set in the HVAC.
2. The ON/OFF behaviour of the HVAC causes the associated temperature T_{aa} to move around the *SP* and the others (T_a, T_{rm}) depending on the former.
3. The hysteresis *ht* with which the HVAC operates also depends on the reference *SP.*
4. The humidity also varies with the operation of HVAC. When the HVAC is in ON mode, it removes humidity from the environment by condensing it on the expansion coil, thus reducing the relative humidity *H* of the environment.
5. When the HVAC is in ON mode and the compressor draws power, the current consumption *I* is almost constant. Thus, a binary signal u_a can be defined as 1 when the HVAC is ON and 0 otherwise, and a relative power P_r as:

$$P_r = \frac{1}{t_p}\int_0^{t_p} u_a\, dt, \text{ with } u_a \in \{0, 1\} \quad \textbf{(4)}$$

where t_p is a specific evaluation time of at least one ON/OFF switching cycle of the HVAC. As a result, P_r ranges between 0 and 1 and is equal to one if the HVAC compressor is always ON (u_a = 1 always). This method of measuring the consumed power makes it possible to be independent of the absolute value of the consumed power [W].

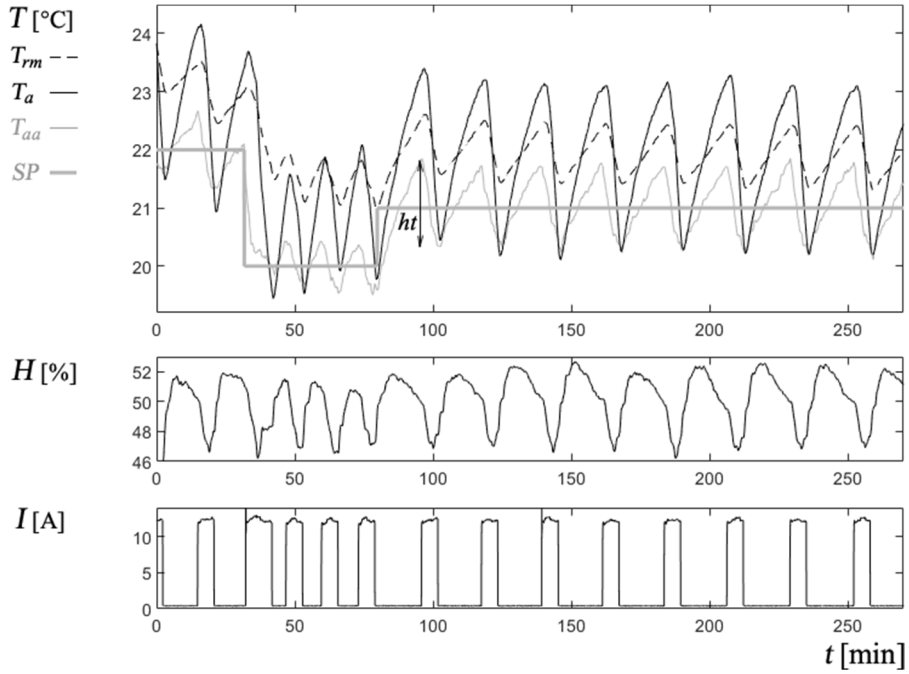

Fig. 15 *Typical behaviour of variables under HVAC action*

3.3.1 INFLUENCE ON TEMPERATURE ASSOCIATED WITH THE HVAC AND THE WALL T_{aa}

This temperature tends to follow the wall temperature due to the outside temperature T_{aaev}, already modelled in 3.2.1, when the HVAC is inactive (OFF mode, $u_a = 0$). On the other hand, if $u_a = 1$ permanently, the wall temperature tends towards the minimum T_{aamin} that the HVAC can reach without switching off the compressor. This value can be obtained by means of a test by setting the *SP* reference to the lowest value it accepts. It depends on the average outdoor temperature. However, it can be considered constant for the summer period under consideration. This is illustrated in the block diagram in Figure 16.

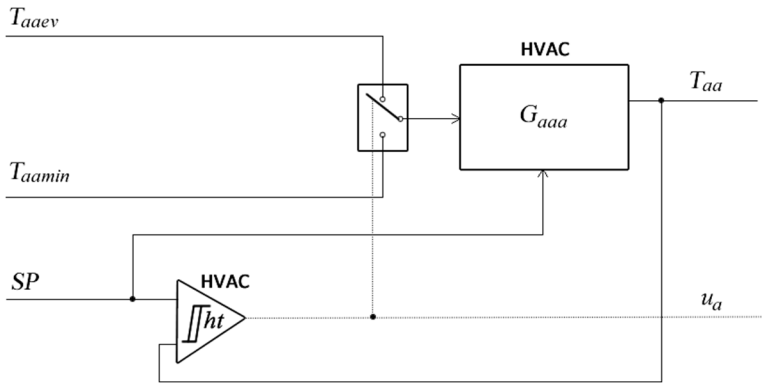

Fig. 16 *Block diagram of the behaviour of the wall temperature associated with the HVAC*

Similar to 3.2, the transfer function G_{aaa} is a first-order LPV system with pure delay similar to (3) but here the parameters vary with the *SP* of the HVAC. A multi-objective identification procedure similar to the one described above was also used to obtain this variation. It is depicted in Figure 17.

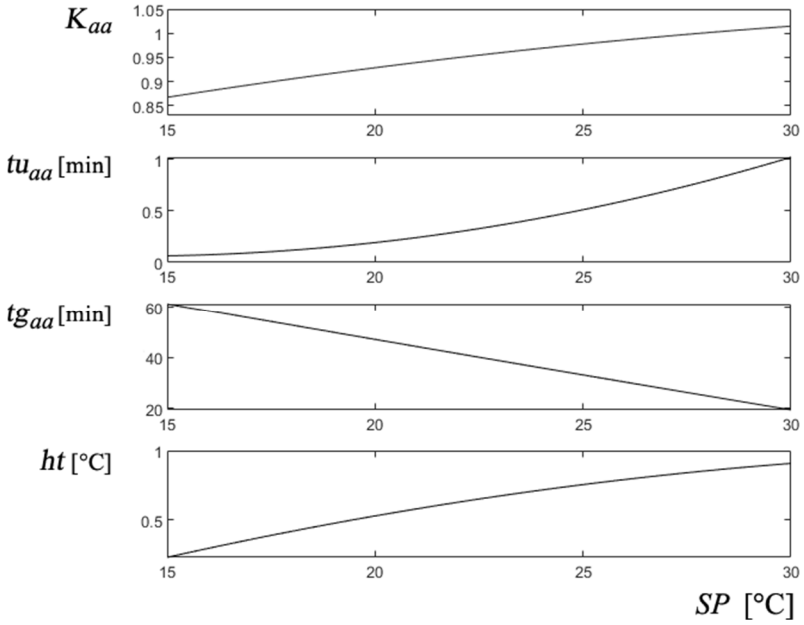

Fig. 17 *Variation of the first-order parameters of G_{aaa} with the SP reference of the HVAC*

3.3.2 INFLUENCE ON THE ROOM TEMPERATURE T_a AND MEAN RADIANT TEMPERATURE T_{rm}

Following the same considerations as in the previous case, the experiments show that when the HVAC is inactive (OFF mode, $u_a = 0$), the ambient temperature tends asymptotically to the wall temperature, which depends only on the outdoor temperature T_{aaev} (see 3.2.1). In the opposite case, when $u_a = 1$, it is determined by the total wall temperature T_{aa} obtained in section 3.3.1 above. This can be represented graphically, as shown in Figure 18.

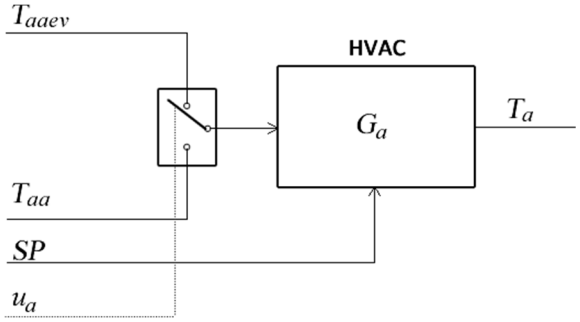

Fig. 18 *Block diagram showing how the ambient temperature T_a depends on the operation of the HVAC*

Again, the corresponding transfer function G_a is a first-order LPV model with pure delay. Its parameters change as a function of the *SP* reference, similarly to those shown for T_{aa} in Figure 17. The behaviour of the mean radiant temperature T_{rm} is similar, although with its parameters.

3.3.3 INFLUENCE ON THE RELATIVE AMBIENT HUMIDITY H

The variations produced by the operation of the HVAC must be added to the H_{aev} humidity produced by the outdoor temperature T_e and the air velocity v_a previously modelled in 3.2.2. This influence was described using a linear system so that:

$$H = H_{aev} + H'_{vc}, \text{ with} \quad \textbf{(5)}$$

$$G_h = \frac{H'_{vc}}{v'_a} = \frac{0.0081\, z^{-75}}{1 - 1.914\, z^{-1} + 0.9154\, z^{-2}}$$

The complete comparison between the measured signals and their models is depicted in Figure 19.

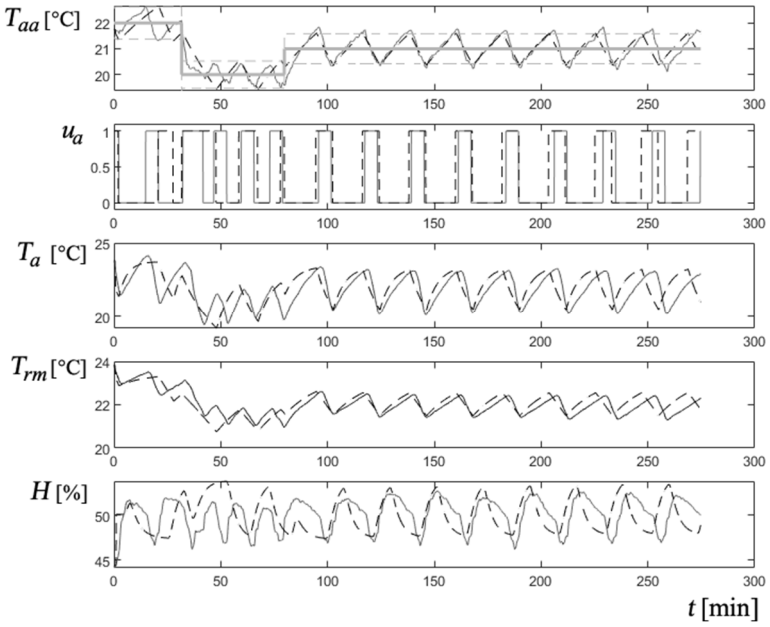

Fig. 19 *Comparison between measured signals and their models, in dashed lines*

3.4. THERMAL COMFORT MODEL

From the modelling of the physical variables described above, a measure of thermal comfort can be derived. The ISO 7730:2005 standard [33] defines it as "that mental condition which expresses satisfaction with the thermal environment" and postulates that up to 10% dissatisfaction with the thermal environment is acceptable. The standard does not provide a way to determine its measure. For this purpose, this study uses the equation proposed by Kuchen et al. [34], which estimates the percentage of dissatisfied users in the environment as follows:

$$Disc = 100 - 93\, exp^{\left(-0{,}0009\,(-T_n+T_{op})^4 - 0{,}034(-T_n+T_{op})^2\right)}\ [\%] \qquad \textbf{(6)}$$

This equation determines users' ability to thermally adapt to the evolution of the indoor climate by incorporating the operative temperature T_{op} and the neutrality temperature T_n, defined below. This model was created based on the correlation of objective and subjective data obtained from 1300 measurements (Spot-Monitoring) in 30 office buildings in central Europe [34,35]. In this model, the minimum possible percentage of dissatisfied users is 7%.

According to the ASHRAE 55 standard [36], the operative temperature T_{op} is an integrated temperature that fully influences the occupant's thermal perception of the thermal environment. The operative temperature is composed of the ambient temperature T_a and the mean radiant temperature T_{rm}, according to the following equation:

$$T_{op} = A\, T_a + (1 - A)\, T_{rm}, \qquad \textbf{(7)}$$

where A is a factor that depends on the v_a air velocity in the environment, as shown in Table 1:

Table 1 *Relationship between the air velocity v_a and the A factor*

v_a [m/s]	$v_a < 0.2$	$0.2 < v_a < 0.6$	$0.6 < v_a < 1$
A	0.5	0.6	0.7

The neutrality temperature T_n is the value at which the individual perceives both physically and psychologically a pleasant environment that is neither cold nor hot. This condition corresponds to a comfort vote $CV = 0$ (neutral) on the 7 points of the ASHRAE 55 scale, as shown in Table 2.

Table 2 *ASHRAE 55 scale*

Thermal sensation	cold	cool	slightly cool	comfortable or neutral	slightly warm	warm	hot
CV	-3	-2	-1	0	1	2	3

There is a linear relationship between the comfort vote and the operative temperature:

$$CV = a\ T_{op} + b \tag{8}$$

Where the parameters a and b can be established determined statistically through user surveys. The T_n neutrality temperature, the T_{op} operative temperature and the CV comfort vote are related by the linear expression:

$$T_n = T_{op} - c\ CV \tag{9}$$

This expression shows that when the operative temperature is neutral, the user should emit a null CV. Constant c was obtained from the survey of the users' comfort votes. For the environment under study, described in section 3.2, these values are $a = 0.3555$, $b = -8.8424$ and $c = 1/b = -0{,}8869$.

From the last equation, it is clear that:

$$-T_n + T_{op} = c\ CV \tag{10}$$

This last value is finally inserted into Eq. (6) to determine the *Disc* percentage of dissatisfied users.

3.4.1 EFFECT OF HUMIDITY ON COMFORT

It is well known that when humidity is high, the air cannot absorb the evaporation on the skin, making it difficult for the body to release heat. This increases the user's sensation of warmth. Another factor that plays a role in this sensation is the speed of air. This has already been taken into account in Eq. (7). To consider the influence of humidity, the concept of thermal sensation or heat index T_{ts} [37] is used. It was first proposed by Steadman [38] in his comfort model and expressed by Rothfusz [39] using the following polynomial form:

$$\begin{aligned} T_{ts} = {} & -8.784695 + 1.61139411\ T_a + 2.33854883889\ H - 0.14611605\ H\ T_a - \\ & 0.012308094\ T_a^2 - 0.0164248277778\ H^2 + 0.002211732\ H T_a^2 + 0.00072546\ T_a\ H^2 - \\ & 0.000003582\ H^2 T_a^2 \quad [°C] \end{aligned} \tag{11}$$

Alternative expressions for the heat index are given in the literature. Stull [40] even cites a third-order polynomial index.

The US National Weather Service [41] warns that this expression is not valid for combinations of high temperatures and humidities and that in certain areas it should be corrected using the following criteria:

If $H < 13\%$ and $26.67°C < T_a < 43°C$ the following adjusting value must be subtracted from (11):

$$Adj = \frac{(13\text{-}H)}{4}\sqrt{\frac{17 - \left|{}^{9}/_{5}T_a - 63\right|}{17}} \quad \textbf{(12)}$$

If $H > 85\%$ and $26.67°C < T_a < 30.55°C$ the following adjustment value must be added to (11):

$$Adj = \frac{(H\text{-}85)}{10}\frac{(54 - {}^{9}/_{5}T_a)}{5} \quad \textbf{(13)}$$

Finally, this simpler expression should be used when the ambient temperature is below 25°C:

$$T_{ts} = [0.15\ (93 + {}^{9}/_{5}\ T_a + 1.2({}^{9}/_{5}\ T_a - 36) + 0.094H) + T_a] / 2 \quad \textbf{(14)}$$

Based on these criteria, the graph of the heat index as a function of ambient temperature and humidity is shaped as shown in Figure 20.

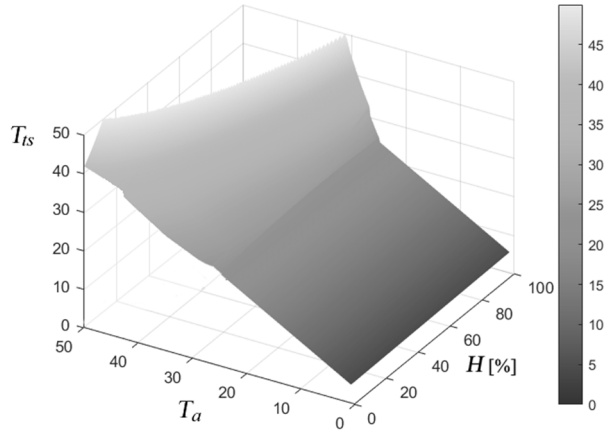

Fig. 20 *Variation of the heat index with ambient temperature and humidity*

It can be seen that the dependence on humidity is minimal as long as $T_a < 25°C$, but above this temperature, the contribution to the heat sensation is large.

To include the heat index in the measurement of the percentage of dissatisfied users *Disc*, it is used instead of the ambient temperature in (7). The result is shown in Figure 21.

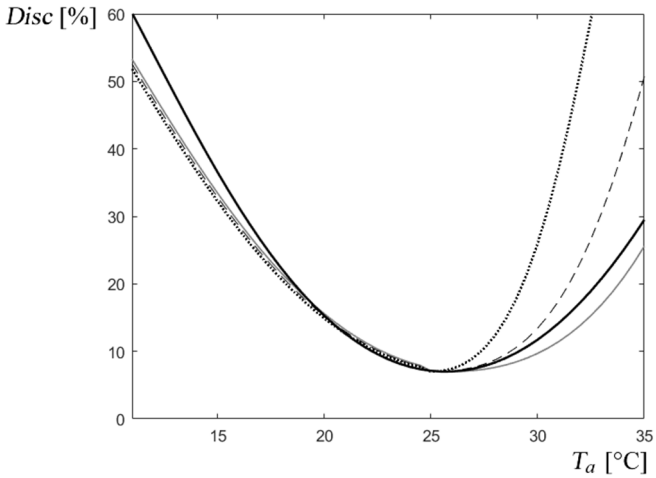

Fig. 21 *Disc variation with ambient temperature and various humidity conditions: Grey line: H = 25%; Dashed line: H = 50%; Dotted line: H = 75%; Full black line: without considering humidity*

In accordance with Fig. 20, the effect of humidity on the percentage of dissatisfied users is minimal at T_a < 25°C but very noticeable above this temperature.

Figure 22 shows the evolution of the percentage of dissatisfied users *Disc,* the ambient temperature T_a and the mean radiant temperature T_{rm}, which are responsible for the behaviour of the former, with a variation in the outside temperature T_e between 20°C and 35°C, typical of the summer season in the area. The v_a air speed was 0.2 m/s and the humidity H was around 40%. The HVAC system was not in operation.

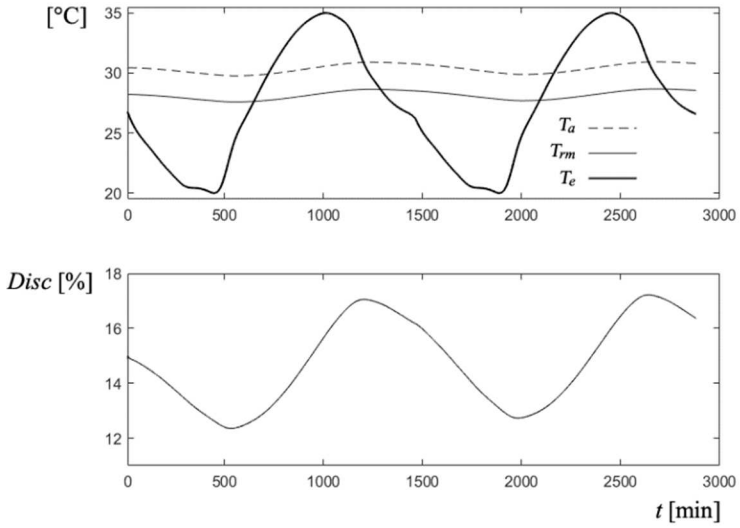

Fig. 22 *Evolution of the Disc percentage of dissatisfied users in a 48hs trial*

4. RESULTS

The model developed enables tests to be carried out to simulate the process under different conditions. Particularly noteworthy are the variables subject to further optimisation, especially the relative power consumption P_r and the percentage of dissatisfied users *Disc*.

Figure 23 shows the behaviour of the wall temperature T_{aa}, which follows the setpoint *SP* over a wide range of temperature references between 15°C and 24°C.

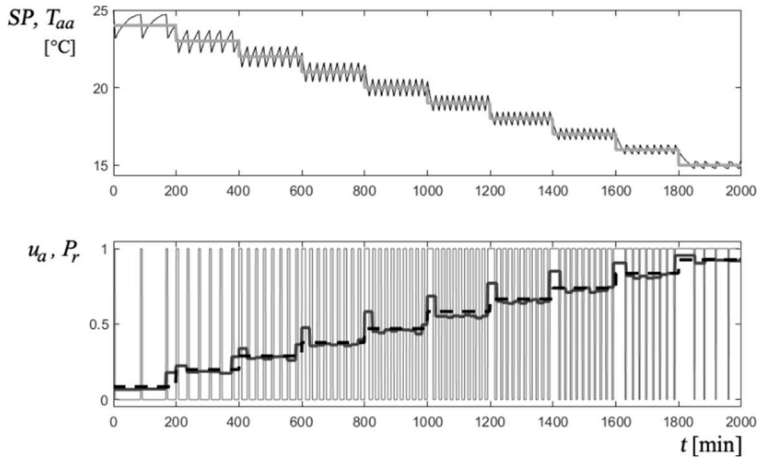

Fig. 23 *SP reference variation test over a wide range*

In this simulated experiment, the outdoor temperature T_e is kept constant to show the almost linear behaviour of the relative power P_r with the setpoint SP.

Two relative powers have been plotted: in the thick grey solid line, the power measured during the period t_p, which considers a single ON/OFF cycle of the HVAC compressor. The dashed line shows the relative power calculated over the period when SP was constant. The bottom graph shows the variation of the ratio between the ON and OFF times of the control signal u_a (thin line) and the progressive increase of the relative power consumption when SP decreases, as expected. As this test is designed to analyse the behaviour of the relative power consumption, the percentage of dissatisfied users, which increases as the temperature drops below the neutral temperature of 25°C, was not plotted.

Figure 24 illustrates a reverse scenario, where the SP reference of the HVAC remains constant at 23°C, and the response to a conventional outdoor temperature variation T_e is observed over 48 hours. The relative power P_r follows a quasi-sinusoidal pattern corresponding to changes in both the ambient temperature T_a and the mean radiant temperature T_{rm}. The same applies to the percentage of dissatisfied users $Disc$, which remains below 10% and is therefore considered acceptable according to current standards.

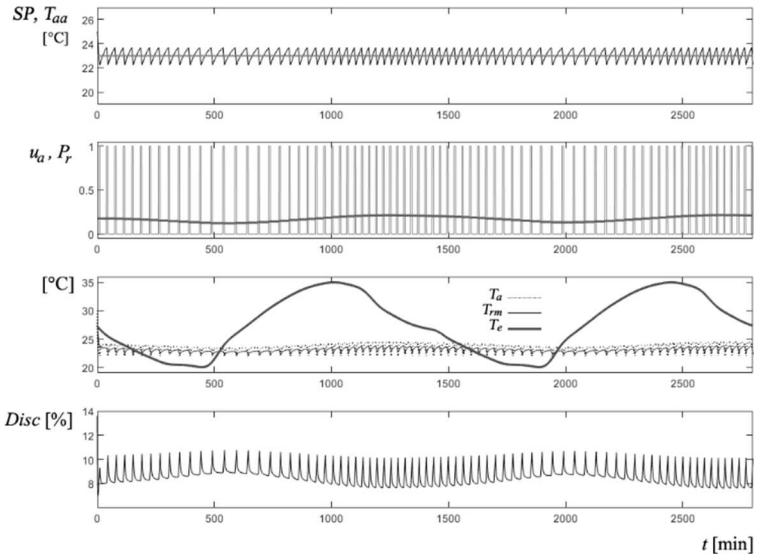

Fig. 24 *System evolution with constant SP reference*

5. CONCLUSIONS

A dynamic grey box model was developed to predict the temporal evolution of temperatures and humidity in a workspace of the UNSJ Faculty of Engineering. The simulated variables follow the measured variables with sufficient accuracy, which makes this model suitable for MPC control. It does not require detailed knowledge of the physical parameters of the various system components, as is common in a theoretical white box model, nor does it require large data packages that completely cover all operating states of the system, as is the case with data-driven black box models. The internal variables involved allow the prediction of the necessary measures for a subsequent MPC multi-objective supervision of the environment climate: the power consumption of the HVAC and the percentage of dissatisfied users with the thermal environment.

Although previous studies have developed grey box models, this study is original and provides new insights because

- It takes into account the internal dependencies between variables.
- It includes relative humidity in the model.
- It uses LPV versions of some sub-models to allow a better description of the non-linear relationships.
- It also considers the effect of forced cross-ventilation from outside, which can help to reduce the power requirements of air-conditioning.
- It defines the relative power of an HVAC in the post-occupancy phase and makes it possible to be independent of the absolute power [W] consumed by the equipment. This facilitates the subsequent optimisation process.
- The methodology for determining the model parameters is straightforward and easily replicable and can therefore be adapted to determine other environments.

Reducing energy costs without compromising the quality of life in the operation of buildings is a public objective, as it contributes to the cost-effective energy transition. Conserving energy resources and reducing environmental impact is a condition to be achieved through sustainable buildings and cities. Applying this dynamic model to optimise the air conditioning of a building with current equipment would not only extend its lifespan but also avoid the tendency to replace it with more efficient equipment.

6. FORTHCOMING DEVELOPMENTS

Using the developed model, the multi-objective predictive supervision technique will be applied to obtain the air speed profile and HVAC setpoint that will be applied to the system.

A strategy will be designed for online updating of the described model is designed. In this way, seasonal variations will be captured better.

7. REFERENCES

[1] J. Verhaart, M. Veselý, W. Zeiler, Personal heating: effectiveness and energy use, *Building Research & Information*, Vol. 43, No. 3, pp. 346–354, 2015.

https://doi.org/10.1080/09613218.2015.1001606

[2] Instituto Argentino de Normalización y Certificación, IRAM 11603 Clasificación bioambiental de la República Argentina, 2021.

[3] B.D. Arballo, E. Kuchen, D. Chuk, Optimización multiobjetivo de la eficiencia energética y el confort térmico en edificios de oficina públicos, Periodo crítico de verano en la ciudad de San Juan, Argentina, *Hábitat Sustentable*, Vol. 12, No. 1, pp. 102–113, 2022.

https://doi.org/10.22320/07190700.2022.12.01.07

[4] Y. Donoso, R. Fabregat, *Multi-Objective Optimization in Computer Networks Using Metaheuristics*, USA: Auerbach Publications, 2007.

[5] E.F. Camacho, C. Bordons, *Model Predictive Control in the Process Industry*, London: Springer-Verlag; 1995.

[6] J. Cígler, D. Gyalistras, J. Široky, et al. Beyond theory: the challenge of implementing model predictive control in buildings, Proceedings of 11th Rehva world congress, Clima, 2013.

[7] A. Afram, F. Janabi-Sharifi. Review of modeling methods for HVAC systems, *Applied Thermal Engineering*, Vol. 67, No. 1-2, pp. 507–519, 2014.

https://doi.org/10.1016/j.applthermaleng.2014.03.055

[8] R.Z. Homod, Review on the HVAC System Modeling Types and the Shortcomings of Their Application, *Journal of Energy*, e768632, 2013.

https://doi.org/10.1155/2013/768632

[9] K. Arendt, M. Jradi, H.R. Shaker, et al. Comparative Analysis of White-, Gray- and Black-box Models for Thermal Simulation of Indoor Environment: Teaching Building Case Study, Proceedings of the 2018 Building Performance Modeling Conference and SimBuild co-organized by ASHRAE and IBPSA-USA, Chicago, IL: ASHRAE; pp. 173–180, 2018.

[10] J.L.M. Hensen, Application of modelling and simulation to HVAC systems, Proceedings of 30th Int. Conf. MOSIS '96, Krnov: Technical University of Ostrava; 1996.

[11] N. Muñoz, L.P. Thomas, B.M. Marino, COMPORTAMIENTO TÉRMICO DINÁMICO DE MUROS TÍPICOS EMPLEANDO EL MÉTODO DE LA ADMITANCIA, *Energías Renovables y Medio Ambiente*, Vol. 36, pp. 31–39, 2015.

[12] B. Tashtoush, M. Molhim, M. Al-Rousan, Dynamic model of an HVAC system for control analysis, *Energy*, Vol. 30, No. 10, pp. 1729–1745, 2005.

https://doi.org/10.1016/j.energy.2004.10.004

[13] I. Beausoleil-Morrison, F. Macdonald, M. Kummert, et al. Co-simulation between ESP-r and TRNSYS, *Journal of Building Performance Simulation*, Vol. 7, No. 2, pp. 133–151, 2014.

https://doi.org/10.1080/19401493.2013.794864

[14] M. Jradi, C.T. Veje, B.N. Jørgensen, A dynamic energy performance-driven approach for assessment of buildings energy Renovation—Danish case studies, *Energy and Buildings*, Vol. 158, pp. 62–76, 2018. https://doi.org/10.1016/j.enbuild.2017.09.094

[15] G.G. Akkurt, N. Aste, J. Borderon, et al. Dynamic thermal and hygrometric simulation of historical buildings: Critical factors and possible solutions. Renewable and Sustainable Energy Reviews, Vol. 118, 109509, 2020. https://doi.org/10.1016/j.rser.2019.109509

[16] S. Prívara, J. Cigler, Z. Váňa, et al. Building modeling as a crucial part for building predictive control, Energy and Buildings, Vol. 56, pp. 8–22, 2013.

https://doi.org/10.1016/j.enbuild.2012.10.024

[17] M. Trcka, J.L.M. Hensen, Overview of HVAC system simulation, Automation in Construction, Vol. 19, No. 2, pp. 93–99, 2010.

https://doi.org/10.1016/j.autcon.2009.11.019

[18] E. Asadi, M.G. da Silva, C.H. Antunes, et al. Multi-objective optimization for building retrofit: A model using genetic algorithm and artificial neural network and an application, *Energy and Buildings*, Vol. 81, pp. 444–456, 2014.

https://doi.org/10.1016/j.enbuild.2014.06.009

[19] Y. Zhou, X. Tian, C. Zhang, et al. Elastic weight consolidation-based adaptive neural networks for dynamic building energy load prediction modelling, *Energy and Buildings*, Vol. 265, 112098, 2022. https://doi.org/10.1016/j.enbuild.2022.112098

[20] J. Drgona, Model Predictive Control with Applications in Building Thermal Comfort Control [Internet], [Bratislava, Eslovaquia]: Slovak University of Technology in Bratislava, Faculty of Chemical and Food Technology, Institute of Information Engineering, Automation; 2017 [cited 2020 Jun 24]. Available from:

https://www.uiam.sk/assets/fileAccess.php?id=1823&type=1

[21] B. Wang, J. Yang, A. Tan, et al. The Application of Fuzzy Logic to Assess the Performance of Participants and Components of Building Information Modeling, *KICEM Journal of Construction Engineering and Project Management*, Vol. 8, No. 4, pp. 1-24, 2018.

[22] J.S. Shamma, An Overview of LPV Systems, In: J. Mohammadpour, C.W. Scherer, editors, *Control of Linear Parameter Varying Systems with Applications* [Internet], Boston, MA: Springer US [cited 2022 Dec 29], pp. 3–26, 2012.

https://doi.org/10.1007/978-1-4614-1833-7_1

[23] International Organization for Standardization, ISO 5151, Non-ducted air conditioners and heat pumps — Testing and rating for performance, 2017.

[24] J. Wu, Z. Xu, F. Jiang, Analysis and development trends of Chinese energy efficiency standards for room air conditioners, *Energy Policy*, Vol. 125, pp. 368–383, 2019.

https://doi.org/10.1016/j.enpol.2018.10.038

[25] Air-Conditioning, Heating, and Refrigeration Institute, ANSI/AHRI 210/240 Standard for Performance Rating of Unitary Air-conditioning & Air-source Heat Pump Equipment, 2017.

[26] International Organization for Standardization, ISO 7726: Ergonomics of the thermal environment - Instruments for measuring physical quantities, 1998.

[27] H. Guo, D. Aviv, M. Loyola, et al. On the understanding of the mean radiant temperature within both the indoor and outdoor environment, a critical review, *Renewable and Sustainable Energy Reviews*, Vol. 117, 109207, 2020.

https://doi.org/10.1016/j.rser.2019.06.014

[28] Y. Zhao, B. Huang, H. Su, et al. Prediction error method for identification of LPV models, *Journal of Process Control*, Vol. 22, No. 1, pp. 180–193, 2012.

https://doi.org/10.1016/j.jprocont.2011.09.004

[29] O.D. Chuk, G.J.E. Scaglia, C.G.R. Medina, The condition number of the static gains matrix as a quality index in LPV IO MIMO multi-objective identification, *International Journal of Modelling, Identification and Control (IJMIC)*, Vol. 35, No. 1, pp. 20-28, 2020.

https://doi.org/10.1504/IJMIC.2020.113293

[30] D. Chuk, G. Rodriguez Medina, E.A. Núñez, et al. A nonlinear correlation-based index to measure independence of sub models in multi-objective identification of MIMO LPV systems, *International Journal of Modelling, Identification and Control (IJMIC)*, Vol. 26, No. 1, pp. 52-58, 2016. https://doi.org/10.1504/IJMIC.2016.077746

[31] O.D. Chuk, C.G. Rodriguez Medina, Identificación multiobjetivo de modelos LPV tipo entrada – salida, Buenos Aires, Argentina; 2023.

[32] C.C. Coello, G.B. Lamont, D.A. van Veldhuizen, *Evolutionary Algorithms for Solving Multi-Objective Problems*, 2nd edition, New York: Springer; 2007.

[33] International Organization for Standardization, ISO 7730, Ergonomics of the thermal environment — Analytical determination and interpretation of thermal comfort using calculation of the PMV and PPD indices and local thermal comfort criteria, 2005.

[34] E. Kuchen, M.N. Fisch, G.E. Gonzalo, et al. Predição do índice de conforto térmico em edificíos de escritório na Alemanha, *Ambient constr.*; Vol. 11, No. 3, pp. 39–53, 2011.

https://doi.org/10.1590/S1678-86212011000300004

[35] E. Kuchen, *Spot-Monitoring zum thermischen Komfort in Bürogebäuden*, Tönning: Der Andere Verlag; 2008.

[36] ASHRAE 55, Thermal environmental conditions for human occupancy, *ASHRAE Inc.*, Atlanta, USA.; 2004.

[37] J.R. Buzan, K. Oleson, M. Huber, Implementation and comparison of a suite of heat stress metrics within the Community Land Model version 4.5. Geoscientific Model Development, Vol. 8, No. 2, pp. 151–170, 2015. https://doi.org/10.5194/gmd-8-151-2015

[38] R.G. Steadman, The Assessment of Sultriness, Part I: A Temperature-Humidity Index Based on Human Physiology and Clothing Science, *Journal of Applied Meteorology and Climatology,* Vol. 18, No. 7, pp. 861–873, 1979.

https://doi.org/10.1175/1520-0450(1979)018<0861:TAOSPI>2.0.CO;2

[39] L.P. Rothfusz, NWS Technical Attachment (SR 90-23), 1990.

[40] R.B. Stull, Meteorology for Scientists and Engineers, Brooks/Cole; 2000.

[41] USA National Weather Service, The Heat Index Equation [Internet], 2022 [cited 2023 Aug 2], Available from: http://www.wpc.ncep.noaa.gov/html/heatindex_equation.shtml